Title
Wnt Signaling Regulates Pulp Volume and Dentin Thickness

Journal
Journal of Bone and Mineral Research, 29(4)

ISSN
0884-0431

Authors
Lim, Won Hee
Liu, Bo
Cheng, Du
et al.

Publication Date
2014-04-01

DOI
10.1002/jbmr.2088

Peer reviewed

HHS Public Access

Author manuscript

J Bone Miner Res. Author manuscript; available in PMC 2015 August 19.

Published in final edited form as:

J Bone Miner Res. 2014 April ; 29(4): 892–901. doi:10.1002/jbmr.2088.

Wnt signaling regulates pulp volume and dentin thickness

Won Hee Lim[1,2], **Bo Liu**[1], **Du Cheng**[1], **Daniel J Hunter**[1], **Zhendong Zhong**[3,4], **Daniel M Ramos**[5], **Bart O Williams**[4], **Paul T Sharpe**[6], **Claire Bardet**[7], **Su-jung Mah**[8], and **Jill A Helms**[1,*]

[1]Division of Plastic and Reconstructive Surgery, Department of Surgery, Stanford School of Medicine, Stanford, CA 94305, USA

[2]Department of Orthodontics, School of Dentistry & Dental Research Institute, Seoul National University, Seoul, Korea

[3]Center for Musculoskeletal Health, Internal Medicine Department, University of California at Davis, Medical Center

[4]Center for Skeletal Disease Research and Laboratory of Cell Signaling and Carcinogenesis, Van Andel Research Institute, Grand Rapids, MI 49503, USA

[5]Department of Orofacial Sciences, University of California at San Francisco, San Francisco, CA

[6]Department of Craniofacial Development, GKT Dental Institute, Kings College London, Guy's Hospital, London Bridge, London, United Kingdom

[7]PRES, Université Paris Descartes, EA 2496 1 rue Maurice Arnoux 92120 Montrouge, France

[8]Department of Orthodontics, Kyung Hee University Hospital at Gangdong, Seoul, Korea

Abstract

Odontoblasts, cementoblasts, ameloblasts and osteoblasts all form mineralized tissues in the craniofacial complex, and all these cell types exhibit active Wnt signaling during postnatal life. We set out to understand the functions of this Wnt signaling, by evaluating the phenotypes of mice in which the essential Wnt chaperone protein, *Wingless* was eliminated. The deletion of Wls was restricted to cells expressing Osteocalcin, which in addition to osteoblasts includes odontoblasts, cementoblasts, and ameloblasts. Dentin, cementum, enamel, and bone all formed in *OCN-Cre;Wls*$^{fl/fl}$ mice but their homeostasis was dramatically affected. The most notable feature was a significant increase in dentin volume and density. We attribute this gain in dentin volume to a Wnt-mediated mis-regulation of Runx2. Normally, Wnt signaling stimulates Runx2, which in turn

*To whom correspondences should be addressed.

Authors Roles

Study design: WHL, BL, and JAH
Data collection: WHL, BL, DC, DJH, DR
Data analysis: WHL, BL, DC, CB and JAH
Drafting manuscript content: WHL, BL, DC, and JAH
Revising manuscript content: WHL, AZ, BW, DR, PS, SJM, and JAH
Approving final version of manuscript: WHL, BL, DC, DJH, AZ, DR, BW, PS, CB, SJM and JAH
JAH takes responsibility for the integrity of the data analysis.

Disclosures

All authors declare that they have no conflicts of interest.

inhibits DSP; this inhibition must be relieved for odontoblasts to differentiate. In *OCN-Cre;Wls*$^{fl/fl}$ mice, Wnt pathway activation is reduced and Runx2 levels decline. The Runx2-mediated repression of DSP is relieved and odontoblast differentiation is accordingly enhanced. This study demonstrates the importance of Wnt signaling in the homeostasis of mineralized tissues of the craniofacial complex.

Keywords

Wnt signaling pathway; dentin; odontoblast; pulp

Introduction

Wnt signals play decisive roles in the development and homeostasis of mineralized tissues, and a key strategy for demonstrating these functions has been to study how gain- and loss-of-function mutations in components of the Wnt signal transduction pathway affect osteogenesis. For example, reductions in Wnt signaling, either by over-expression of Wnt antagonists, a deficiency of Wnt ligands, or mutations in genes encoding Wnt receptors cause bone loss in humans and in mice (1-3). Conversely, enhancement of Wnt signaling results in increased bone volume, abnormal bone density (i.e., hyperostosis), and pathological thickening of bone, a condition known as sclerosing bone dysplasia (4-7). Wnt signaling also influences the program of odontogenesis, but much less is understood about its role in this complex process. For example, Wnt signaling controls morphological aspects of tooth development including the number (8), the size (9), the position (10), and the shapes (11-15), of teeth (reviewed in (16)). Loss-of-function experiments suggest that Wnt signals regulate the maturation of dental mesenchyme into dentin-secreting odontoblasts (12) and bone-secreting cementoblasts (17) but conflicting reports also exist (18).

Much less are known about the postnatal functions of Wnt signaling in maintaining mineralized tissue homeostasis. Although Wnt signaling remains a critical regulator of bone homeostasis throughout life (19,20), the function of postnatal Wnt signaling in the maintenance of dental mineralized tissues is unclear. A standard knock-out approach to abrogate Wnt signaling is complicated by the fact that there are nineteen, closely related mammalian Wnt genes that are largely redundant (21-23). To overcome this difficulty we made use of a Cre-LoxP system to conditionally delete *Wntless (Wls)*, a chaperone protein that escorts lipid-modified Wnt from the Golgi to the cell surface (24). When *Wls* is inactivated, the secretion of all mammalian Wnt proteins is blocked (24,25) and Wnt signaling is abrogated (26). To block Wnt signaling specifically in mineralized tissues, *Wls*$^{fl/fl}$ mice were crossed with *OCN-Cre* mice to generate *OCN-Cre;Wls*$^{fl/fl}$ offspring (27). Osteocalcin is a major non-collagenous protein synthesized by osteoblasts, odontoblasts, ameloblasts, and cementoblasts (28). Consequently, these mice allowed us to focus on how loss of Wnt protein secretion from cells affects mineralized tissues in the head, regardless of whether they originated from somatic mesoderm, paraxial cephalic mesoderm, or cranial neural crest (29,30).

Materials and Methods

Generation of OCN-Cre;Wls$^{fl/fl}$ mice

The generation of *OCN-Cre;Wls$^{fl/fl}$* mice were performed after review and approval by the Van Andel Research Institute IACUC (protocol #13-03-015). Both *OCN-Cre* and *Wls$^{fl/fl}$* mice are available at Jackson Laboratories (129S-Wls$^{tm1.1Lan}$/J, 012888 for *Wls$^{fl/fl}$* and B6N PVB-Tg1Clem/J,019509 for *OCN-Cre*). Genomic DNA was prepared from tail biopsies using an AutoGenprep 960 automated DNA isolation system (AutoGen). PCR-based strategies were used to genotype the mice (details are available upon request). Thirty mice were analyzed; 10 were 1 month old and 20 were 3 months old.

Generation of Axin2$^{LacZ/+}$ mice; detection of beta galactosidase activity

The generation of *Axin2$^{LacZ/+}$* mice (Jackson Laboratories 129P2-*Axin2^{tm1Wbm}*/J) was performed in accordance with animal welfare based on an approved IACUC protocol #13146 from Stanford University. Ten mice at age of 2 months old were used in this study. Cells responsive to Wnt signaling express the LacZ gene product, beta-galactosidase. Beta galactosidase is then detected by X-gal staining (31). To perform X-gal staining, tissues were fixed in 0.4% paraformaldehyde overnight before being decalcified with 19% EDTA and infused with 30% sucrose for 24hr. Samples were embedded in optimum cutting temperature (OCT) medium and cryosectioned at a thickness of 8 microns. Tissues were then fixed in 0.2% gluteraldehyde for 15min and stained with X-gal overnight at 37°C.

Micro-CT analyses

Micro-CT was performed on 10 mice at the age of 3 months (5 wild-type, 5 *OCN-Cre;Wls$^{fl/fl}$* littermates) using Imtek/Siemens MicroCAT II/SPECT system (Siemens, Knoxville, TN) with at 80kV and 400 micro-amperes and the resolution of 40 microns. Scans of the skulls were acquired using a 6400μm^3 isotropic voxel size, with 650 CT slices evaluated per skull. To determine the mineralized bone fraction, the threshold was standardized with the bone/water/air phantom for each sample. Individual CT slices were reconstructed with COBRA reconstruction software, and data were analyzed with GE Microview (GE Healthcare, Waukesha, WI). The frontal, parietal and occipital bones were selected automatically with the threshold within the region of interest including each of the area.

Micro-CT analyses of the teeth in 10 mice at the age of 3 months (5 wild-type, 5 *OCN-Cre;Wls$^{fl/fl}$* littermates) were taken using MicroXCT-200 (SkyScan, Belgium) with at 60kV and 7.98 Watt and the resolution of 2 microns. Scans were acquired using 8μm^3 isotropic voxel size, with 800 CT slices evaluated in incisor area. For analyses, individual CT slices were reconstructed with MicroXCT7.0 reconstruction software (SkyScan, Belgium), and data were analyzed with Inveon Research Workplace (IRW) (Erlangen, Germany).

Sample preparation, processing and histology

Maxillae from 1-month-old mice (5 wild-type, 5 *OCN-Cre;Wls$^{fl/fl}$* littermates) and 3-month old mice (6 wild-type, 6 *OCN-Cre;Wls$^{fl/fl}$* littermates) were harvested and fixed in 4% paraformaldehyde overnight at 4°C. Samples were decalcified in a heat-controlled

microwave in 19% EDTA for two weeks. After demineralization, specimens were dehydrated through an ascending ethanol series prior to paraffin embedding. Eight-micron-thick longitudinal sections were cut and collected on Superfrost-plus slides for histology.

In situ hybridization

Tissue sections were deparaffinized following standard procedures. Relevant digoxigenin-labeled mRNA antisense probes were prepared from complementary DNA templates for *Osteocalcin*, *Axin2* and *Osterix*. Sections were dewaxed, treated with proteinase K, and incubated in hybridization buffer containing the relevant RNA probe. Probe was added at an approximate concentration of 1 μg/ml. Stringency washes of saline sodium citrate solution were done at 65°C and further washed in maleic acid buffer with 1% Tween 20. Slides were treated with an antibody to Anti-digoxigenin-AP (Roche). For color detection, slides were incubated in nitro blue tetrazolium chloride (Roche) and 5-bromo-4-chloro-3-indolyl phosphate (Roche). After developing, the slides were coverslipped with permount mounting medium.

Histology

Movat's pentachrome staining was performed (32). Nuclei stain blue to black, cytoplasm stains red, collagen stains yellow to greenish yellow, and fibrous tissue stains an intense red. Tissues were also stained with the acidic dye, Picrosirius red (33), to discriminate tightly packed and aligned collagen molecules. Under polarized light, well-aligned fibrillary collagen molecules present polarization colors of longer wavelengths (red) as compared to less organized collagen fibrils that show colors of shorter wavelengths (green-yellow).

Immunohistochemistry

Tissue sections were deparaffinized following standard procedures. Endogenous peroxidase activity was quenched by 3% hydrogen peroxide for 5 min, and then washed in PBS. Slides were blocked with 5% goat serum (Vector S-1000) for 1 hour at room temperature. The appropriate primary antibody was added and incubated overnight at 4°C, then washed in PBS. Samples were incubated with appropriate biotinylated secondary antibodies (Vector BA-x) for 30 minutes, and washed in PBS. An advidin/biotinylated enzyme complex (Kit ABC Peroxidase Standard Vectastain PK-4000) was added and incubated for 30 minutes and a DAB substrate kit (Kit Vector Peroxidase subtrate DAB SK-4100) was used to develop the color reaction. Antibodies used include Ki67 (Thermo Scientific, dilution 1: 100), Runx2 (Origene, dilution 1: 200), Osteopontin (NIH LF 175, dilution 1: 4000), dentin sialoprotein (DSP, Millipore, dilution 1: 2000), dentin phosphoprotein (DPP, which was generated by the Department of Dental Science for Health Promotion, Division of Cervico Gnathostomatology, Hiroshima University, dilution 1: 2000). Counterstain was performed with hematoxylin after development with a DAB substrate in order to count cells.

Quantitative real time-PCR

Dental pulp tissues were carefully removed from formalin-fixed paraffin-embedded (FFPE) tissue and transferred into the processing plate. RNA isolation was carried out using FFPE RNA Isolation kit (Ambion, Austin, USA). Digestion buffer, protease and RNA digestion

additives were added into the processing plate and incubated 60°C for 45 min and 80°C for 30 min. Nucleic acid binding beads were added to the samples, then placed on a titer shaker for 3 min; afterwards, the supernatant was removed. Beads were washed again and the supernant was again removed. Samples were treated with Dnase at 37°C for 20 min; beads were washed, and the supernatant was removed. RNA was quantified using a Nanodrop spectrophotometer (Thermo Fischer scientific, Delaware USA). cDNA was synthesized using Superscript first-strand synthesis supermix following the manufacturers instructions (Life technologies, Austin, USA). Quantitative RT-PCR was performed as described (34). Expression levels were calculated using the 2ˆ-(ddCt) method, normalized to GAPDH (35) and converted to fold-expression. The following primer sets were used: GAPDH, forward primer (ACCCAGAAGACTGTGGATGG) and reverse primer (GGATGCAGGGATGATGTTCT). Runx2, forward primer (ATCGCCTCAGTGATTTAGGG) and reverse primer (TGCCTGGGATCTGTAATCTG). DSP, forward primer (TGGCTGTGCCTCTTCTAACA) and reverse primer (GCTGTTGCTAGTGGTGCTGT).

Statistical analyses

Results are presented as the mean ± SD. Student's t-test was used to quantify differences described in this article. One asterisk (*) denotes a p value of less than .05, and two asterisks (**) denotes a p value of less than .01.

Results

Skeletal tissues have a universal requirement for Wnt signaling

In a first study we demonstrated that Cre-mediated recombination in *OCN-Cre* mice occurred in bone (36). Here, examination of the craniofacial skeleton of *OCN-Cre;Wls*$^{fl/fl}$ mice revealed that similar to the appendicular and axial skeleton, deletion of *Wls* caused a dramatic reduction in bone volume and bone mineral density of both cranial neural crest-derived skeletal elements (bone volume: p <0.01; bone density: p <0.05; Fig. 1A,B) and mesoderm-derived skeletal elements (bone volume and bone density: p <0.01; Fig. 1C,D; quantified in E). Deletion of *Wls*, however, did not affect the size of the skeletal elements (Supplemental Fig. 1).

Unlike the dramatic skeletal phenotype, the dentition of *OCN-Cre;Wls*$^{fl/fl}$ mice was largely intact. For example, the overall size, shape, and position of the teeth was equivalent between wild-type and *OCN-Cre;Wls*$^{fl/fl}$ mice (Fig. 1F,G and Supplemental Fig. 2A,B). The gross morphology of the molars (Fig. 1H,I) and incisors (Fig. 1J,K) was similar in wild-type and mutant mice. We confirmed that in addition to its expression in osteoblasts, *Osteocalcin* is also expressed by ameloblasts that form enamel (Fig. 2B and (37)), by cementoblasts that line the root surface (Fig. 2C and (38,39)), by odontoblasts that produce dentin (40-42), and by pulp cells that maintain the stroma of the pulp cavity (Fig. 2D and (43)). In addition, the expression of *Osteocalcin* in the inner enamel epithelium was first clearly observed at E18.5.

Postnatal ameloblasts, odontoblasts, and pulp cells are Wnt-responsive

Given the *Osteocalcin* expression patterns and the fact that Wnt signaling is implicated in the development of each of these dental tissues, we more closely examined the dentition in *OCN-Cre;Wls*$^{fl/fl}$ mice for anomalies resulting from a disruption of Wnt signaling. We focused on the incisors of *OCN-Cre;Wls*$^{fl/fl}$ mice and in a separate, ongoing study we evaluated the molar phenotypes.

Using a 2μm-resolution micro-CT, reconstructions of the incisors revealed that removal of *Wls* in *Osteocalcin*-expressing ameloblasts resulted in increased enamel production (arrows, Fig. 2E, F) without disrupting the overall size or shape of the incisor (Supplemental Fig. 2). Normally, enamel covers about 75% of the buccal incisor surface; in *OCN-Cre;Wls*$^{fl/fl}$ mice enamel covered about 90% of the surface. Transverse micro-CT sections near the incisor apex (dotted lines, Fig. 2E, F) illustrated this point: mineralized enamel is normally detected ~1.43 μm from the root apex; regions closer to the apex therefore lack enamel in wild-type (Fig. 2G). In *OCN-Cre;Wls*$^{fl/fl}$ mice, however, more apical sections showed a well-mineralized enamel matrix (arrow, Fig. 2H). This gain in enamel mineralization stood in sharp contrast to the thin alveolar bone surrounding the *OCN-Cre;Wls*$^{fl/fl}$ incisor (asterisks, Fig. 2G,H).

Removal of *Wls* from odontoblasts also resulted in a significant gain in mineralized tissue formation. The total volume of the tooth remained constant between wild-type and *OCN-Cre;Wls*$^{fl/fl}$ specimens ($p = .08$ at root apex and $p = .06$ at incisive edge; Fig. 2I,J; quantified in K; see also Supplemental Fig. 2C,D) but serial sections through the incisor clearly showed that in *OCN-Cre;Wls*$^{fl/fl}$ mice, the percentage of tooth structure occupied by dentin was significantly increased ($p < .01$; Fig. 2L,M; quantified in K). This increase in dentin volume was compensated by a reduction in pulp volume in *OCN-Cre;Wls*$^{fl/fl}$ mice, most obviously at the incisive edge (dotted circle, $p < .01$; Fig. 2L,M; quantified in K; see also Supplemental Fig. 2B). The molecular mechanisms underlying this gain in dentin volume became the focus of our next experiments.

Adult odontoblasts and pulp cells maintain their dependency on endogenous Wnt signaling

The gain in dentin volume we observed in *OCN-Cre;Wls*$^{fl/fl}$ mice is predicated on odontoblasts maintaining a dependency on Wnt signaling into adulthood. Previous reports, however, suggest that after postnatal day 15, molar odontoblasts and odontoblasts at the incisor tip lose their Wnt responsiveness (44). We revisited this issue of adult odontoblast dependency on a Wnt signal using the same strain of Wnt reporter (e.g., *Axin2*$^{LacZ/+}$) mice and cryo-sectioned tissues from 2-months old mice. We found that both incisor tip odontoblasts and pulp fibroblasts were X-gal positive (Fig. 3A,B). We examined the other mineralizing dental tissues and confirmed the Wnt-responsive status of cementoblasts (Fig. 3C,D), ameloblasts (Fig. 3E,F), and osteoblasts (Fig. 3G,H) in skeletally mature *Axin2*$^{LacZ/+}$ mice. Thus, all mineralizing tissues in the craniofacial complex maintain their Wnt-responsive status into adulthood.

Differential regulation of Runx2 mediates *OCN*-Cre;Wls$^{fl/fl}$ bone loss and dentin gain

We sought to reconcile two apparently disparate findings, that reduced Wnt signaling in *OCN-Cre;Wls*$^{fl/fl}$ mice simultaneously produces a loss in bone volume (Fig. 1) and a gain in dentin volume (Fig. 2). We first verified that Wnt signaling was reduced in the pulp of *OCN-Cre;Wls*$^{fl/fl}$ mice, using expression of the Wnt target gene *Axin2* as a readout of pathway activity (45,46). Compared to its expression in wild-type osteoblasts, *Axin2* expression was reduced to nearly undetectable levels in *OCN-Cre;Wls*$^{fl/fl}$ osteoblasts (Fig. 4A,B). A similar reduction in *Axin2* expression was observed in *OCN-Cre;Wls*$^{fl/fl}$ odontoblasts (compare wild-type, Fig. 4C with D).

Despite the significantly increased dentin volume, the organization of the dentin matrix in *OCN-Cre;Wls*$^{fl/fl}$ mice appeared to be the same as in wild-type mice (Fig. 5A, B), although the density of the dentin was significantly increased in *OCN-Cre;Wls*$^{fl/fl}$ mice (Fig. 5C). Ki67 immunostaining was non-existent in the pulp cavities of both wild-type and mutant mice (Fig. 5D, E), so it was unlikely that the increased dentin volume was attributable to differences in proliferation of *OCN-Cre;Wls*$^{fl/fl}$ odontoblasts. We also examined the protein expression of DPP, DSP, Osteopontin, Osterix, and Runx2 (Supplemental Fig. 3) and of these dentin markers, we only noticed a difference in Runx2 expression levels.

Compared to wild-type odontoblasts, the protein was noticeably reduced in *OCN-Cre;Wls*$^{fl/fl}$ odontoblasts (Fig. 5F,J). Using immunostaining and cell nuclei counting, we observed significantly higher level of Runx2 expression in wild-type mice compared to *OCN-Cre;Wls*$^{fl/fl}$ mice (Fig. 5 H), although we observed statistically insignificant change in qRT-PCR. Concomitant with Runx2 down regulation, DSP expression was markedly increased in *OCN-Cre;Wls*$^{fl/fl}$ odontoblasts (Fig. 5I,J). Using qRT-PCR, we showed a statistically significant, 1.7 fold increase in DSP expression in the *OCN-Cre;Wls*$^{fl/fl}$ mice(Fig. 5K). This is in keeping with reports demonstrating that Runx2 negatively regulates the differentiation of cells into odontoblasts (47) via inhibition of dentin sialoprotein (DSP; (47)). Taken together, the loss in bone volume and the gain in dentin volume caused by the reduction of Wnt signaling in *OCN-Cre;Wls*$^{fl/fl}$ mice can be jointly explained by reduced Runx2 expression. In osteoblasts, a reduction in Runx2 results in an arrest in differentiation; conversely, reduced Runx2 expression in odontoblasts results in an acceleration in differentiation.

Discussion

We used a conditional loss-of-function strategy to test the requirement for Wnt signaling in mineralized tissue homeostasis. In examining the skeleton of *OCN-Cre;Wls*$^{fl/fl}$ mice we found that regardless of embryonic origin, function, or role in weight bearing, all bones appeared to be equally affected by the loss of Wls (Fig. 1 and see (36). Thus, there appears to be a universal requirement for Wnt signaling for the maintenance of bone mineral density and bone volume, a conclusion strongly supporting by the existing literature (48). There is not, however, a corresponding, well-defined role for Wnt signaling in odontogenesis. This became the subject of our investigation.

A reduction in Wnt signaling is associated with a gain in dentin formation

Wnt signaling controls tooth shape, size, position and number; consequently, we anticipated that *OCN-Cre;Wls*$^{fl/fl}$ mice would exhibit a tooth-related phenotype. We were surprised to discover that there was no overt disruption in odontogenesis (Figs. 1, 2; Supplemental Fig. 2). Micro-CT reconstructions revealed that instead of a loss, there was actually a gain in dentin volume (Fig. 2). How could a reduction in Wnt signaling simultaneously lead to bone loss, and dentin accumulation?

We initially suspected that the negative impact of Wls removal did not extend to odontoblasts and pulp cells because of the conditional nature of the deletion. We verified, however, that adult odontoblasts and pulp cells, as well as ameloblasts and osteoblasts expressed *Osteocalcin* (Fig. 2 and see (43)). Therefore, these cell types would be subjected to Wls deletion in *OCN-Cre;Wls*$^{fl/fl}$ mice.

We then wondered if dental tissues escaped the negative effects of Wls removal, because Wnt responsiveness is thought to be a feature of fetal and early post-natal odontoblasts but not of adult cells (44). We used the same *Axin2*$^{LacZ/+}$ reporter mice as Lohi and colleagues but instead of paraffin embedding, used cryo-embedding. In these adult tissues X-gal staining clearly revealed odontoblasts, pulp fibroblasts, ameloblasts, and cementoblasts, along with periodontal ligament cells all maintained their Wnt responsive status into adulthood (Fig. 3). Therefore, odontoblasts and pulp cells require Wnt signaling and in *OCN-Cre;Wls*$^{fl/fl}$ mice, the requisite Wnt signal would not be secreted and both cell types would be devoid of this stimulus.

Wls-deficient cells maintain their ability to respond to a Wnt stimulus (A.Z and B.O.W., unpublished observations); therefore, it is formally possible that *OCN-Cre;Wls*$^{fl/fl}$ odontoblasts and pulp cells still receive- and respond- to a Wnt signal and thus the increased mineral density is not related to decreased Wnt signaling. The reduced *Axin2* expression in the mutant pulp cavity, however, argues against this possibility (Fig. 4). Thus, we conclude that whatever its source, Wnt signaling is abrogated in the pulp cavity of *OCN-Cre;Wls*$^{fl/fl}$ mice, and this reduction in Wnt signaling is directly responsible for a gain in dentin formation.

Wnt regulates Runx2 in osteoblasts and odontoblasts

The function of Runx2 in the differentiation of odontoblasts and osteoblasts is still a point of much debate (reviewed in (49)). Initially, Runx2/Cbfa1 was thought to specifically regulate osteoblast maturation (50) but this was eventually disproven. Investigators have since demonstrated key roles for Runx2 in chondrocyte maturation (51) as well as many other cell types (52). Thesleff and colleagues were the first to identify a function for Runx2 in odontoblasts, where its action appeared to inhibit the maturation process (53). New insights into the function of Runx2 came with the discovery that Wnt signaling promotes osteogenesis by stimulating Runx2 activity (54) but whether it also serves as positive stimulus in odontoblasts has not been resolved. We showed that Wnt-deficient *OCN-Cre;Wls*$^{fl/fl}$ osteoblasts have reduced Runx2 expression (Supplemental Fig. 3 G, H) and that reduced Runx2 expression is accompanied by reduced Osteocalcin expression and dramatic

bone loss (Fig. 1 and see Supplemental Fig. 3 I, J). Wnt-deficient *OCN-Cre;Wls*$^{fl/fl}$ odontoblasts also exhibit reduced Runx2 expression (Fig. 5), but then the differentiation process diverges: Reduced Runx2 expression in *OCN-Cre;Wls*$^{fl/fl}$ odontoblasts is accompanied by an increase in DSP expression (Fig. 5) with no significant change in Osteocalcin expression (Supplemental Fig. 3 K, L). When these data are considered together, they support a model whereby Wnt signaling acts a positive stimulus for Runx2 expression in both odontoblasts and osteoblasts, but its transcriptional activity in these two cell types differs: In osteoblasts, Runx2 drives maturation, whereas in odontoblasts Runx2 appears to inhibit differentiation. This interpretation is in keeping with other reports examining the function of Runx2 in mineralizing tissues (53).

Does Wnt signaling regulate odontoblast differentiation?

OCN-Cre;Wls$^{fl/fl}$ mice exhibit stronger DSP expression and they have denser dentin (Fig. 5); presently the mechanisms behind this increase in dentin density are unknown. There are two plausible explanations: first, each odontoblast in *OCN-Cre;Wls*$^{fl/fl}$ mice could secrete more dentin than a wild-type odontoblast. Alternatively, pulp cells in *OCN-Cre;Wls*$^{fl/fl}$ mice might differentiate into odontoblasts more readily than wild-type pulp cells. The latter hypothesis is particularly intriguing because it provides a means by which to explain an increase in dentin volume without a commensurate increase in cell proliferation. If true, then pulp cells located in the subodontoblastic layer (55) of *OCN-Cre;Wls*$^{fl/fl}$ mice may be responsible for generating more dentin, even without an injury stimulus (56). A simple histologic examination of the subodontoblastic layer in wild-type and *OCN-Cre;Wls*$^{fl/fl}$ mice, however, did not reveal any notable alterations so this hypothesis remains a speculation at the current time. Nonetheless, a role for Wnt signaling in the activation of progenitor cells that contribute to the repair of a mineralized tissue has indirect support from data on bone healing (57), and may well be involved in odontogenic repair as well.

Wnt signaling and cellular aging of the dental pulp

Throughout life odontoblasts continue to secrete an extracellular matrix that becomes mineralized (58-60) and as a consequence the pulp chamber narrows with age (61). The molecular regulation of this process is unknown. We observe an exaggerated version of this same process in *OCN-Cre;Wls*$^{fl/fl}$ mice: the pulp chamber reduces while the dentin gradually thickens (Fig. 2). Simultaneous with this gain in mineralized dentin we observe a profound loss in bone mass in *OCN-Cre;Wls*$^{fl/fl}$ mice (62), which is also a hallmark of human aging (63,64). In other work, we demonstrated that aging is associated with a decline in Wnt signaling, specifically in the bone marrow cavity (65). Coupled with new data demonstrating that Wnt signaling regulates telomerase activity (66,67), which is tightly correlated with a decline in osteogenesis and the onset of cellular senescence (68,69). It is tempting to speculate that some of the changes we observe in the *OCN-Cre;Wls*$^{fl/fl}$ dentition are an exaggerated version of an aging phenotype brought about by a gradual loss of Wnt signaling (70). If this hypothesis holds true, some age-related effects on mineralized tissues of the body may be treatable via a Wnt-based approach.

Supplementary Material

Refer to Web version on PubMed Central for supplementary material.

Acknowledgments

This research project was supported by a grant from the California Institute of Regenerative Medicine (CIRM) TR1-0219 and NIH ROI AR053293. Micro XCT imaging work was performed at the Division of Biomaterials and Bioengineering Micro-CT Imaging Facility, UCSF, supported by NIH Grant S10RR026645, and the Departments of Preventive and Restorative Dental Sciences and Orofacial Sciences, School of Dentistry, UCSF.

References

1. Kim JB, Leucht P, Lam K, Luppen C, Ten Berge D, Nusse R, Helms JA. Bone regeneration is regulated by wnt signaling. J Bone Miner Res. 2007; 22(12):1913–23. [PubMed: 17696762]
2. Bennett CN, Longo KA, Wright WS, Suva LJ, Lane TF, Hankenson KD, MacDougald OA. Regulation of osteoblastogenesis and bone mass by Wnt10b. Proc Natl Acad Sci U S A. 2005; 102(9):3324–9. [PubMed: 15728361]
3. Gong Y, Slee RB, Fukai N, Rawadi G, Roman-Roman S, Reginato AM, Wang H, Cundy T, Glorieux FH, Lev D, Zacharin M, Oexle K, Marcelino J, Suwairi W, Heeger S, Sabatakos G, Apte S, Adkins WN, Allgrove J, Arslan-Kirchner M, Batch JA, Beighton P, Black GC, Boles RG, Boon LM, Borrone C, Brunner HG, Carle GF, Dallapiccola B, De Paepe A, Floege B, Halfhide ML, Hall B, Hennekam RC, Hirose T, Jans A, Juppner H, Kim CA, Keppler-Noreuil K, Kohlschuetter A, LaCombe D, Lambert M, Lemyre E, Letteboer T, Peltonen L, Ramesar RS, Romanengo M, Somer H, Steichen-Gersdorf E, Steinmann B, Sullivan B, Superti-Furga A, Swoboda W, van den Boogaard MJ, Van Hul W, Vikkula M, Votruba M, Zabel B, Garcia T, Baron R, Olsen BR, Warman ML. LDL receptor-related protein 5 (LRP5) affects bone accrual and eye development. Cell. 2001; 107(4):513–23. [PubMed: 11719191]
4. Morvan F, Boulukos K, Clement-Lacroix P, Roman Roman S, Suc-Royer I, Vayssiere B, Ammann P, Martin P, Pinho S, Pognonec P, Mollat P, Niehrs C, Baron R, Rawadi G. Deletion of a single allele of the Dkk1 gene leads to an increase in bone formation and bone mass. J Bone Miner Res. 2006; 21(6):934–45. [PubMed: 16753024]
5. Little RD, Carulli JP, Del Mastro RG, Dupuis J, Osborne M, Folz C, Manning SP, Swain PM, Zhao SC, Eustace B, Lappe MM, Spitzer L, Zweier S, Braunschweiger K, Benchekroun Y, Hu X, Adair R, Chee L, FitzGerald MG, Tulig C, Caruso A, Tzellas N, Bawa A, Franklin B, McGuire S, Nogues X, Gong G, Allen KM, Anisowicz A, Morales AJ, Lomedico PT, Recker SM, Van Eerdewegh P, Recker RR, Johnson ML. A mutation in the LDL receptor-related protein 5 gene results in the autosomal dominant high-bone-mass trait. Am J Hum Genet. 2002; 70(1):11–9. [PubMed: 11741193]
6. Boyden LM, Mao J, Belsky J, Mitzner L, Farhi A, Mitnick MA, Wu D, Insogna K, Lifton RP. High bone density due to a mutation in LDL-receptor-related protein 5. N Engl J Med. 2002; 346(20): 1513–21. [PubMed: 12015390]
7. Babij P, Zhao W, Small C, Kharode Y, Yaworsky PJ, Bouxsein ML, Reddy PS, Bodine PV, Robinson JA, Bhat B, Marzolf J, Moran RA, Bex F. High bone mass in mice expressing a mutant LRP5 gene. J Bone Miner Res. 2003; 18(6):960–74. [PubMed: 12817748]
8. Wang XP, O'Connell DJ, Lund JJ, Saadi I, Kuraguchi M, Turbe-Doan A, Cavallesco R, Kim H, Park PJ, Harada H, Kucherlapati R, Maas RL. Apc inhibition of Wnt signaling regulates supernumerary tooth formation during embryogenesis and throughout adulthood. Development. 2009; 136(11):1939–49. [PubMed: 19429790]
9. Sarkar L, Sharpe PT. Inhibition of Wnt signaling by exogenous Mfrzb1 protein affects molar tooth size. J Dent Res. 2000; 79(4):920–5. [PubMed: 10831093]
10. Sarkar L, Cobourne M, Naylor S, Smalley M, Dale T, Sharpe PT. Wnt/Shh interactions regulate ectodermal boundary formation during mammalian tooth development. Proc Natl Acad Sci U S A. 2000; 97(9):4520–4.

11. Liu F, Chu EY, Watt B, Zhang Y, Gallant NM, Andl T, Yang SH, Lu MM, Piccolo S, Schmidt-Ullrich R, Taketo MM, Morrisey EE, Atit R, Dlugosz AA, Millar SE. Wnt/beta-catenin signaling directs multiple stages of tooth morphogenesis. Dev Biol. 2008; 313(1):210–24. [PubMed: 18022614]
12. Zhang R, Yang G, Wu X, Xie J, Yang X, Li T. Disruption of Wnt/beta-catenin signaling in odontoblasts and cementoblasts arrests tooth root development in postnatal mouse teeth. Int J Biol Sci. 2013; 9(3):228–36. [PubMed: 23494738]
13. Kim TH, Bae CH, Lee JC, Ko SO, Yang X, Jiang R, Cho ES. beta-catenin is required in odontoblasts for tooth root formation. J Dent Res. 2013; 92(3):215–21. [PubMed: 23345535]
14. Han XL, Liu M, Voisey A, Ren YS, Kurimoto P, Gao T, Tefera L, Dechow P, Ke HZ, Feng JQ. Post-natal effect of overexpressed DKK1 on mandibular molar formation. J Dent Res. 2011; 90(11):1312–7. [PubMed: 21917600]
15. Kratochwil K, Galceran J, Tontsch S, Roth W, Grosschedl R. FGF4, a direct target of LEF1 and Wnt signaling, can rescue the arrest of tooth organogenesis in Lef1(-/-) mice. Genes Dev. 2002; 16(24):3173–85. [PubMed: 12502739]
16. Thesleff I. Epithelial-mesenchymal signalling regulating tooth morphogenesis. J Cell Sci. 2003; 116(Pt 9):1647–8. [PubMed: 12665545]
17. Kim TH, Lee JY, Baek JA, Lee JC, Yang X, Taketo MM, Jiang R, Cho ES. Constitutive stabilization of ss-catenin in the dental mesenchyme leads to excessive dentin and cementum formation. Biochem Biophys Res Commun. 2011; 412(4):549–55. [PubMed: 21854758]
18. Nemoto E, Koshikawa Y, Kanaya S, Tsuchiya M, Tamura M, Somerman MJ, Shimauchi H. Wnt signaling inhibits cementoblast differentiation and promotes proliferation. Bone. 2009
19. Leucht P, Minear S, Ten Berge D, Nusse R, Helms JA. Translating insights from development into regenerative medicine: the function of Wnts in bone biology. Semin Cell Dev Biol. 2008; 19(5): 434–43. [PubMed: 18824114]
20. Minear S, Leucht P, Jiang J, Liu B, Zeng A, Fuerer C, Nusse R, Helms JA. Wnt proteins promote bone regeneration. Sci Transl Med. 2010; 2(29):29ra30.
21. Yamamoto Y, Takeshita H, Sawa H. Multiple Wnts redundantly control polarity orientation in Caenorhabditis elegans epithelial stem cells. PLoS Genet. 2011; 7(10):e1002308. [PubMed: 22022276]
22. Farin HF, Van Es JH, Clevers H. Redundant sources of Wnt regulate intestinal stem cells and promote formation of Paneth cells. Gastroenterology. 2012; 143(6):1518–1529 e7. [PubMed: 22922422]
23. Najdi R, Proffitt K, Sprowl S, Kaur S, Yu J, Covey TM, Virshup DM, Waterman ML. A uniform human Wnt expression library reveals a shared secretory pathway and unique signaling activities. Differentiation. 2012; 84(2):203–13. [PubMed: 22784633]
24. Banziger C, Soldini D, Schutt C, Zipperlen P, Hausmann G, Basler K. Wntless, a conserved membrane protein dedicated to the secretion of Wnt proteins from signaling cells. Cell. 2006; 125(3):509–22. [PubMed: 16678095]
25. Bartscherer K, Pelte N, Ingelfinger D, Boutros M. Secretion of Wnt ligands requires Evi, a conserved transmembrane protein. Cell. 2006; 125(3):523–33. [PubMed: 16678096]
26. Fu J, Jiang M, Mirando AJ, Yu HM, Hsu W. Reciprocal regulation of Wnt and Gpr177/mouse Wntless is required for embryonic axis formation. Proc Natl Acad Sci U S A. 2009; 106(44): 18598–603. [PubMed: 19841259]
27. Carpenter AC, Rao S, Wells JM, Campbell K, Lang RA. Generation of mice with a conditional null allele for Wntless. Genesis. 2010; 48(9):554–8. [PubMed: 20614471]
28. Bronckers AL, Price PA, Schrijvers A, Bervoets TJ, Karsenty G. Studies of osteocalcin function in dentin formation in rodent teeth. Eur J Oral Sci. 1998; 106(3):795–807. [PubMed: 9672102]
29. Couly GF, Coltey PM, Le Douarin NM. The triple origin of skull in higher vertebrates: a study in quail-chick chimeras. Development. 1993; 117(2):409–29. [PubMed: 8330517]
30. Le Douarin NM. Piecing together the vertebrate skull. Development. 2012; 139(23):4293–6. [PubMed: 23132239]
31. Burn SF. Detection of beta-galactosidase activity: X-gal staining. Methods Mol Biol. 2012; 886:241–50. [PubMed: 22639266]

32. Movat HZ. Demonstration of all connective tissue elements in a single section; pentachrome stains. AMA Arch Pathol. 1955; 60(3):289–95. [PubMed: 13248341]
33. Whittaker P, Kloner RA, Boughner DR, Pickering JG. Quantitative assessment of myocardial collagen with picrosirius red staining and circularly polarized light. Basic Res Cardiol. 1994; 89(5):397–410. [PubMed: 7535519]
34. Leucht P, Jiang J, Cheng D, Liu B, Dhamdhere G, Fang MY, Monica SD, Urena JJ, Cole W, Smith LR, Castillo AB, Longaker MT, Helms JA. Wnt3a reestablishes osteogenic capacity to bone grafts from aged animals. J Bone Joint Surg Am. 2013; 95(14):1278–88. [PubMed: 23864176]
35. Livak KJ, Schmittgen TD. Analysis of relative gene expression data using real-time quantitative PCR and the 2(-Delta Delta C(T)) Method. Methods. 2001; 25(4):402–8. [PubMed: 11846609]
36. Zhong Z, Zylstra-Diegel CR, Schumacher CA, Baker JJ, Carpenter AC, Rao S, Yao W, Guan M, Helms JA, Lane NE, Lang RA, Williams BO. Wntless functions in mature osteoblasts to regulate bone mass. Proc Natl Acad Sci U S A. 2012
37. Gluhak-Heinrich J, Guo D, Yang W, Harris MA, Lichtler A, Kream B, Zhang J, Feng JQ, Smith LC, Dechow P, Harris SE. New roles and mechanism of action of BMP4 in postnatal tooth cytodifferentiation. Bone. 2010; 46(6):1533–45. [PubMed: 20206312]
38. Du Y, Ling J, Wei X, Ning Y, Xie N, Gu H, Yang F. Wnt/beta-catenin signaling participates in cementoblast/osteoblast differentiation of dental follicle cells. Connect Tissue Res. 2012; 53(5): 390–7. [PubMed: 22360497]
39. Xie H, Liu H. A novel mixed-type stem cell pellet for cementum/periodontal ligament-like complex. J Periodontol. 2012; 83(6):805–15. [PubMed: 22014173]
40. Hoffmann M, Olson K, Cavender A, Pasqualini R, Gaikwad J, D'Souza RN. Gene expression in a pure population of odontoblasts isolated by laser-capture microdissection. J Dent Res. 2001; 80(11):1963–7. [PubMed: 11759003]
41. Towler DA, Bidder M, Latifi T, Coleman T, Semenkovich CF. Diet-induced diabetes activates an osteogenic gene regulatory program in the aortas of low density lipoprotein receptor-deficient mice. J Biol Chem. 1998; 273(46):30427–34. [PubMed: 9804809]
42. Sommer B, Bickel M, Hofstetter W, Wetterwald A. Expression of matrix proteins during the development of mineralized tissues. Bone. 1996; 19(4):371–80. [PubMed: 8894143]
43. Papagerakis P, Berdal A, Mesbah M, Peuchmaur M, Malaval L, Nydegger J, Simmer J, Macdougall M. Investigation of osteocalcin, osteonectin, and dentin sialophosphoprotein in developing human teeth. Bone. 2002; 30(2):377–85. [PubMed: 11856645]
44. Lohi M, Tucker AS, Sharpe PT. Expression of Axin2 indicates a role for canonical Wnt signaling in development of the crown and root during pre- and postnatal tooth development. Dev Dyn. 2010; 239(1):160–7. [PubMed: 19653310]
45. Jho EH, Zhang T, Domon C, Joo CK, Freund JN, Costantini F. Wnt/beta-catenin/Tcf signaling induces the transcription of Axin2, a negative regulator of the signaling pathway. Mol Cell Biol. 2002; 22(4):1172–83. [PubMed: 11809808]
46. Lustig B, Jerchow B, Sachs M, Weiler S, Pietsch T, Karsten U, van de Wetering M, Clevers H, Schlag PM, Birchmeier W, Behrens J. Negative feedback loop of Wnt signaling through upregulation of conductin/axin2 in colorectal and liver tumors. Mol Cell Biol. 2002; 22(4):1184–93. [PubMed: 11809809]
47. Miyazaki T, Kanatani N, Rokutanda S, Yoshida C, Toyosawa S, Nakamura R, Takada S, Komori T. Inhibition of the terminal differentiation of odontoblasts and their transdifferentiation into osteoblasts in Runx2 transgenic mice. Arch Histol Cytol. 2008; 71(2):131–46. [PubMed: 18974605]
48. Baron R, Kneissel M. WNT signaling in bone homeostasis and disease: from human mutations to treatments. Nat Med. 2013; 19(2):179–92. [PubMed: 23389618]
49. Komori T. Regulation of osteoblast and odontoblast differentiation by Runx2. Journal of Oral Biosciences. 2010; 52(1):22–25.
50. Thirunavukkarasu K, Mahajan M, McLarren KW, Stifani S, Karsenty G. Two domains unique to osteoblast-specific transcription factor Osf2/Cbfa1 contribute to its transactivation function and its inability to heterodimerize with Cbfbeta. Mol Cell Biol. 1998; 18(7):4197–208. [PubMed: 9632804]

51. Yoshida CA, Komori T. Role of Runx proteins in chondrogenesis. Crit Rev Eukaryot Gene Expr. 2005; 15(3):243–54. [PubMed: 16390320]
52. Ferrari N, McDonald L, Morris JS, Cameron ER, Blyth K. RUNX2 in mammary gland development and breast cancer. J Cell Physiol. 2013; 228(6):1137–42. [PubMed: 23169547]
53. James MJ, Jarvinen E, Wang XP, Thesleff I. Different roles of Runx2 during early neural crest-derived bone and tooth development. J Bone Miner Res. 2006; 21(7):1034–44. [PubMed: 16813524]
54. Gaur T, Lengner CJ, Hovhannisyan H, Bhat RA, Bodine PV, Komm BS, Javed A, van Wijnen AJ, Stein JL, Stein GS, Lian JB. Canonical WNT signaling promotes osteogenesis by directly stimulating Runx2 gene expression. J Biol Chem. 2005; 280(39):33132–40. [PubMed: 16043491]
55. Gotjamanos T. Cellular organization in the subodontoblastic zone of the dental pulp. I. A study of cell-free and cell-rich layers in pulps of adult rat and deciduous monkey teeth. Arch Oral Biol. 1969; 14(9):1007–10. [PubMed: 4981474]
56. Harada M, Kenmotsu S, Nakasone N, Nakakura-Ohshima K, Ohshima H. Cell dynamics in the pulpal healing process following cavity preparation in rat molars. Histochem Cell Biol. 2008; 130(4):773–83. [PubMed: 18463888]
57. Whyte JL, Smith AA, Helms JA. Wnt signaling and injury repair. Cold Spring Harb Perspect Biol. 2012; 4(8):a008078. [PubMed: 22723493]
58. Foster BL, Nagatomo KJ, Tso HW, Tran AB, Nociti FH Jr, Narisawa S, Yadav MC, McKee MD, Millan JI, Somerman MJ. Tooth root dentin mineralization defects in a mouse model of hypophosphatasia. J Bone Miner Res. 2013; 28(2):271–82. [PubMed: 22991301]
59. Sakai VT, Zhang Z, Dong Z, Neiva KG, Machado MA, Shi S, Santos CF, Nor JE. SHED differentiate into functional odontoblasts and endothelium. J Dent Res. 2010; 89(8):791–6. [PubMed: 20395410]
60. Arana-Chavez VE, Massa LF. Odontoblasts: the cells forming and maintaining dentine. Int J Biochem Cell Biol. 2004; 36(8):1367–73. [PubMed: 15147714]
61. Lee YH, Kim GE, Cho HJ, Yu MK, Bhattarai G, Lee NH, Yi HK. Aging of in vitro pulp illustrates change of inflammation and dentinogenesis. J Endod. 2013; 39(3):340–5. [PubMed: 23402504]
62. Zhong Z, Zylstra-Diegel CR, Schumacher CA, Baker JJ, Carpenter AC, Rao S, Yao W, Guan M, Helms JA, Lane NE, Lang RA, Williams BO. Wntless functions in mature osteoblasts to regulate bone mass. Proc Natl Acad Sci U S A. 2012; 109(33):E2197–204. [PubMed: 22745162]
63. Gabet Y, Bab I. Microarchitectural changes in the aging skeleton. Curr Osteoporos Rep. 2011; 9(4):177–83. [PubMed: 21901426]
64. Boskey AL, Coleman R. Aging and bone. J Dent Res. 2010; 89(12):1333–48. [PubMed: 20924069]
65. Leucht P, Jiang J, Liu B, Cheng D, Monica S, Urena J, Dhamdhere G, Fang M, Helms JA. Wnt3a reverse the fatty degeneration of aged bone marrow through its control of mesenchymal stem cell fate. Journal of Bone and Joint Surgery. In press.
66. Hoffmeyer K, Raggioli A, Rudloff S, Anton R, Hierholzer A, Del Valle I, Hein K, Vogt R, Kemler R. Wnt/beta-catenin signaling regulates telomerase in stem cells and cancer cells. Science. 2012; 336(6088):1549–54. [PubMed: 22723415]
67. Zhang Y, Toh L, Lau P, Wang X. Telomerase reverse transcriptase (TERT) is a novel target of Wnt/beta-catenin pathway in human cancer. J Biol Chem. 2012
68. Gronthos S, Chen S, Wang CY, Robey PG, Shi S. Telomerase accelerates osteogenesis of bone marrow stromal stem cells by upregulation of CBFA1, osterix, and osteocalcin. J Bone Miner Res. 2003; 18(4):716–22. [PubMed: 12674332]
69. Bernardes de Jesus B, Blasco MA. Telomerase at the intersection of cancer and aging. Trends Genet. 2013
70. Iyer S, Ambrogini E, Bartell SM, Han L, Roberson PK, de Cabo R, Jilka RL, Weinstein RS, O'Brien CA, Manolagas SC, Almeida M. FOXOs attenuate bone formation by suppressing Wnt signaling. J Clin Invest. 2013; 123(8):3409–19. [PubMed: 23867625]

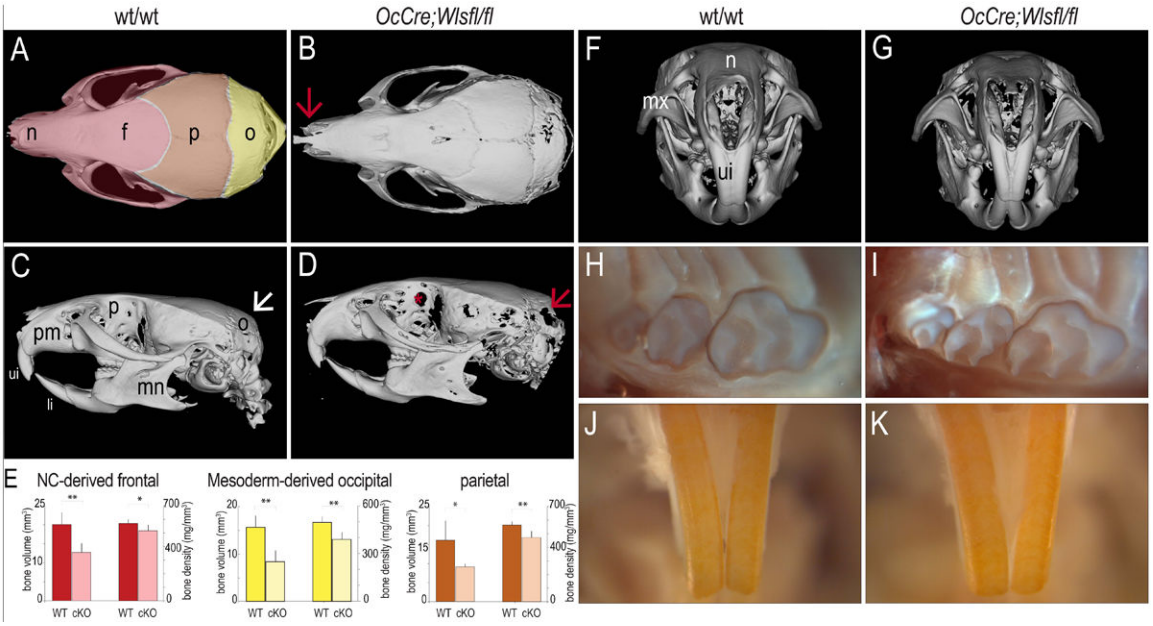

Fig.1. Down regulation of Wnt signaling results in reduced bone density in skeleton but intact dentition of OCN-Cre;Wls$^{fl/fl}$ mice

(A, B) The deletion of Wls causes significant reduction in bone volume and bone density of *OCN-Cre;Wls$^{fl/fl}$* frontal bone. (C, D) Substantially reduced bone volume and bone density are observed in *OCN-Cre;Wls$^{fl/fl}$* parietal and occipital bones. (E) Quantification reveals a statistically significant reduction in bone volume and bone density in *OCN-Cre;Wls$^{fl/fl}$* craniofacial skeleton. (F, G) Overall volume of the teeth is equivalent between the wild-type and *OCN-Cre;Wls$^{fl/fl}$* mice. (H, I) Gross morphology and appearance of molars are equivalent between the wild-type and *OCN-Cre;Wls$^{fl/fl}$* mice. (J, K) Wild-type and *OCN-Cre;Wls$^{fl/fl}$* incisors appear to have equivalent size and appearance. * $p < .05$ *and* ** $p < .01$.

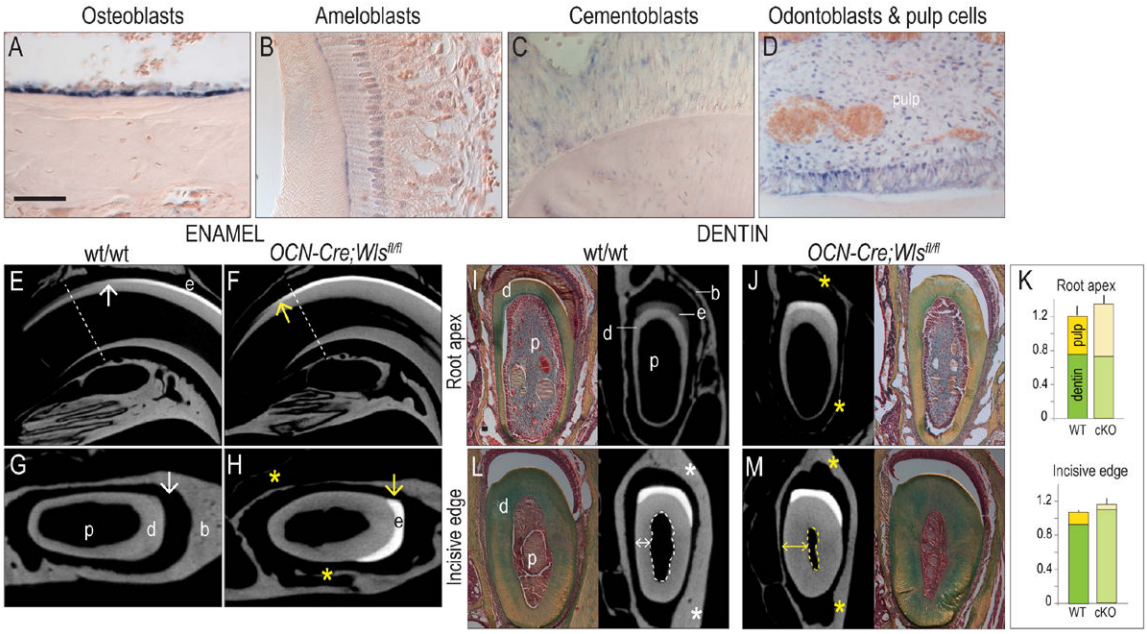

Fig.2. A disruption of Wnt signaling causes anomalies in the OCN-Cre;Wls$^{fl/fl}$ mineralized dental tissues

(A) Osteoblasts, (B) ameloblasts, (C) cementoblast and (D) odontoblast and pulp cells of 3 months old wild-type mice show osteocalcin expression (purple color). The brown color is produced by red blood cells due to abundant iron porphyrin complexes. (E, F) In 3 months old *OCN-Cre;Wls$^{fl/fl}$* mice, enamel covers more root surface including near the incisor apex than wild-type mice. (G, H) Wild-type mice lack enamel in region closer to the apex, while *OCN-Cre;Wls$^{fl/fl}$* mice has a well-mineralized enamel but thin alveolar bone surrounding the incisor. (I, J) The total volume of the tooth remains constant between wild-type and *OCN-Cre;Wls$^{fl/fl}$* mice. (L, M) The dentin volume is significantly increased in *OCN-Cre;Wls$^{fl/fl}$* mice near the incisive edge. (K) Quantification reveals equivalent tooth volume but a statistically significant increase in dentin volume in *OCN-Cre;Wls$^{fl/fl}$* mice. Scale bar: (A-D) 50μm, (I-M) 50μm.

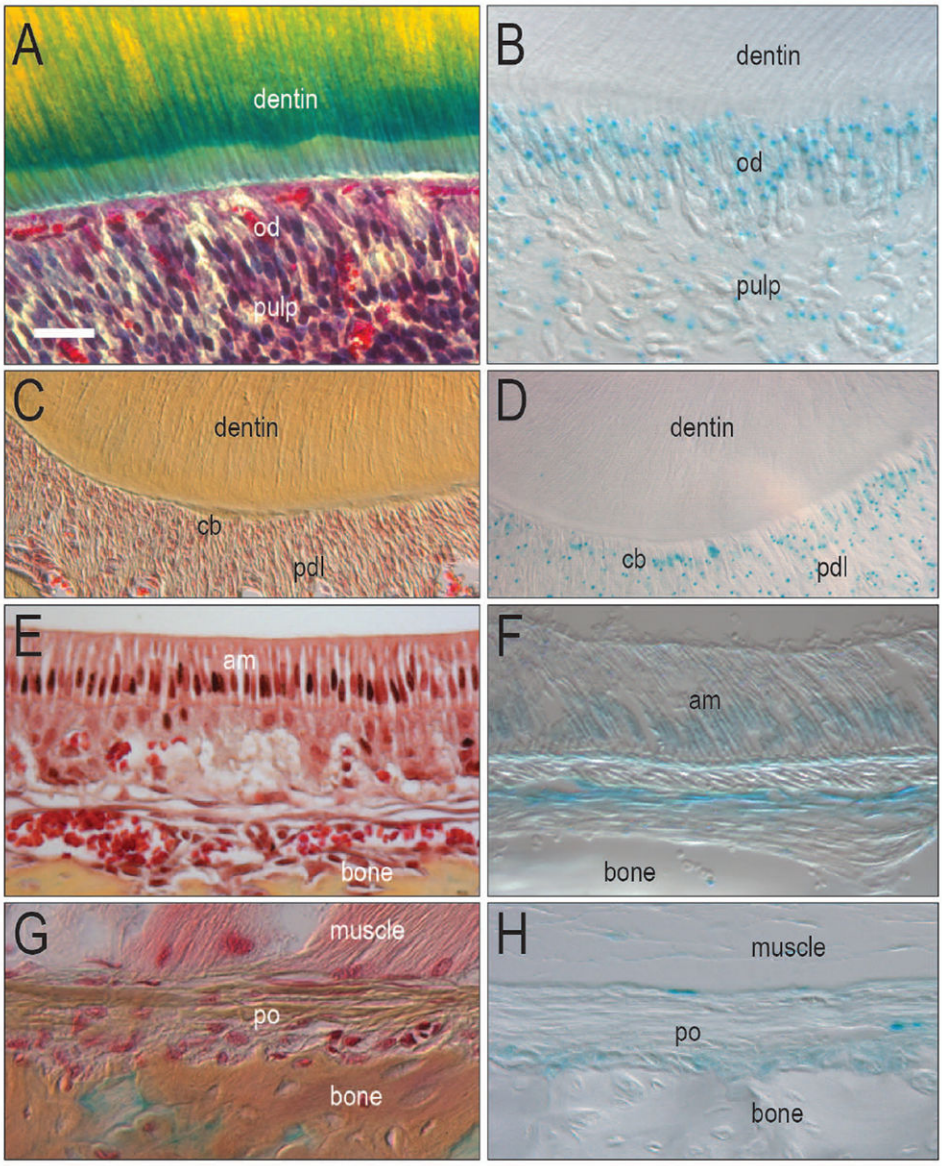

Fig.3. Wnt responsiveness is maintained until adulthood

(A, B) Odontoblasts and pulp fibroblasts in 2-month old *Axin2*$^{LacZ/+}$ incisors are X-gal staining positive. (C, D) Cementoblasts, (E, F) ameloblasts and (G, H) osteoblasts are Wnt-responsive in 2-month old *Axin2*$^{LacZ/+}$ mice. Scale bar: (A-D) 50μm.

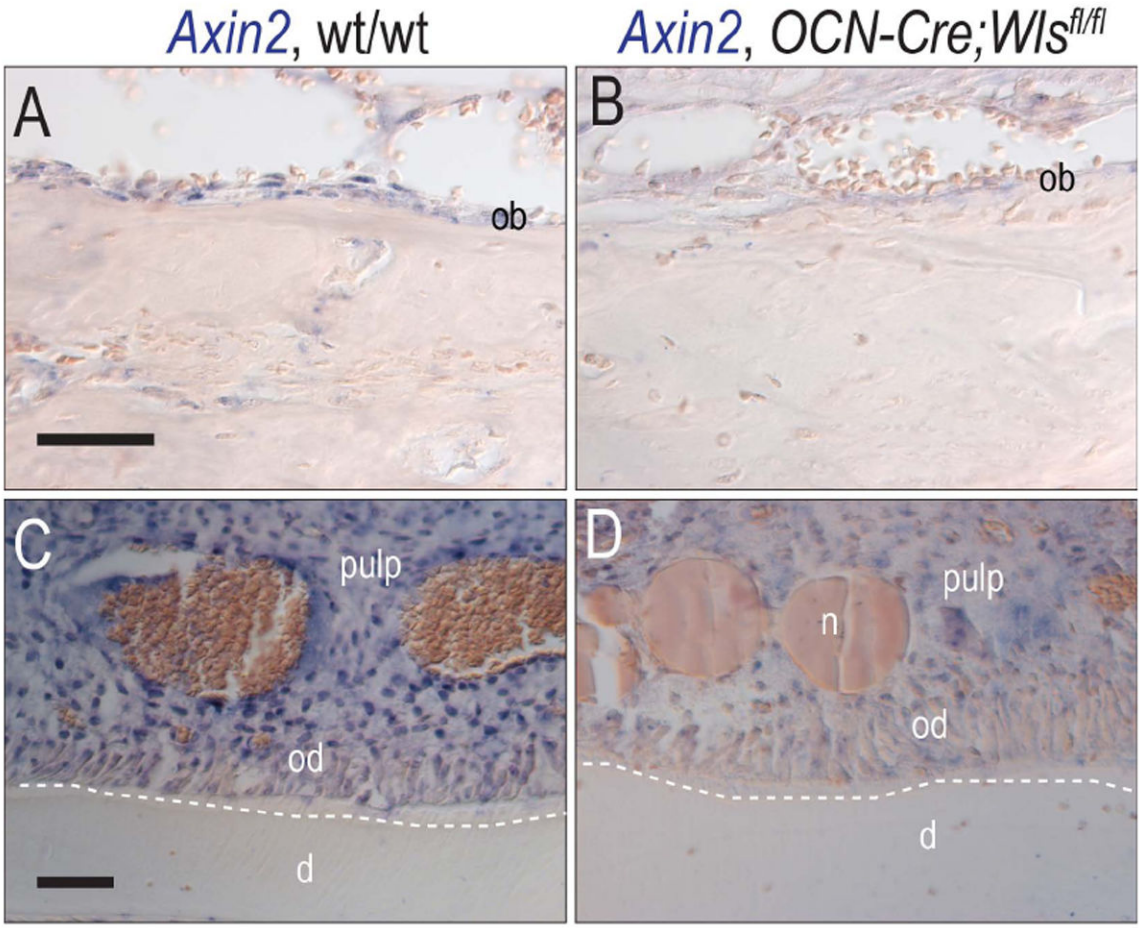

Fig.4. Down regulation of Wnt signaling results in reduction of Axin2 expression

(A, B) Expression of *Axin2* is reduced in *OCN-Cre;Wls*$^{fl/fl}$ osteoblasts compared to wild-type osteoblasts. (C, D) Odontoblasts in *OCN-Cre;Wls*$^{fl/fl}$ mice shows reduction of *Axin2* expression compared to wild-type mice. Scale bar: (A, B) 50μm, (C, D) 50μm.

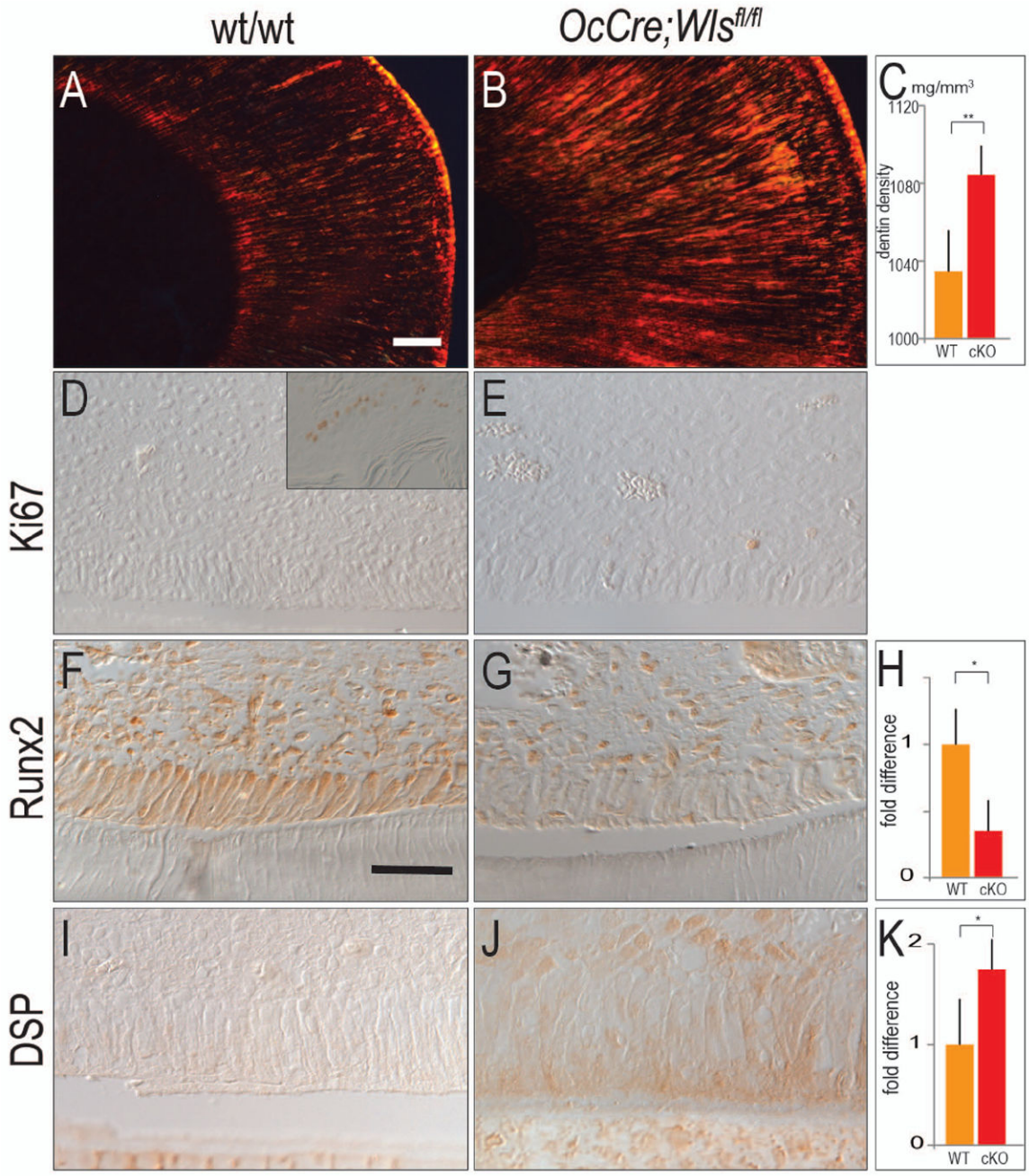

Fig.5. Bone loss and dentin gain in OCN-Cre;Wls$^{fl/fl}$ mice result from Runx2 alteration

(A, B) Picrosirius red staining shows similar dentin matrix organization between wild-type and *OCN-Cre;Wls$^{fl/fl}$* mice. (C) *OCN-Cre;Wls$^{fl/fl}$* mice has significantly denser dentin compared to wild-type mice. (D, E) Ki67 expression shows no difference in cell proliferation of odontoblasts and pulp between wild-type and *OCN-Cre;Wls$^{fl/fl}$* mice. The small figure in (D) shows Ki67 expression in rugae area. (F, G) Significantly reduced Runx2 expression is observed in *OCN-Cre;Wls$^{fl/fl}$* odontoblasts and pulp. (H) Using immunostaining and cell nuclei counting, significantly higher level of Runx2 was observed in wild-type mice compared to *OCN-Cre;Wls$^{fl/fl}$* mice (unit, fold difference relative to WT).

(I, J) DSP expression is considerably increased in odontoblasts and pulp of *OCN-Cre;Wls*$^{fl/fl}$ mice. (K) Using qRT-PCR, DSP expression in *OCN-Cre;Wls*$^{fl/fl}$ mice is significantly higher than wild-type mice (unit, fold difference relative to WT). ** $p < .01$. Scale bar: (A, B, D, E, I, J) 50μm, (F, G) 50μm.